Estimation of the particle–wall interaction energy in sedimentation field flow fractionation[☆]

Nikolaos Lioris, Lambros Farmakis, Athanasia Koliadima, George Karaiskakis[*]

Department of Chemistry, University of Patras, Panepistimioupoli Rion, GR-26504 Patras, Greece

Available online 7 March 2005

Abstract

A new sedimentation field flow fractionation (SdFFF) method is presented for the estimation of the total potential energy of interaction between colloidal particles and the channel wall. The method is based on the variation of the mean cloud thickness in SdFFF to the variation of the suspension's ionic strength. It requires only two SdFFF experiments at two different ionic strengths and at a constant acceleration field. The found values are compatible with those calculated from the various forms of equations of the Derjaguin–Landau–Verwey–Overbeek (DLVO) theory.
© 2005 Published by Elsevier B.V.

Keywords: Potential energy; Particle–wall interaction; Sedimentation field flow fractionation; Potential barrier field flow fractionation; Field flow fractionation; Cloud thickness

1. Introduction

Field flow fractionation (FFF) is classified as a one-phase chromatographic technique in which an externally adjusted force field is applied to the suspended particles under motion in a channel [1–4]. Sedimentation field flow fractionation (SdFFF) is one FFF subtechnique where a centrifugal force field is used as the external field. The theoretical basis of SdFFF makes possible the calculation of particle mass, diameter, density and related properties for uncharacterized colloidal particles based on experimentally measured retention parameters [5–8]. When the retention ratio is calculated, the particle–wall and particle–particle interactions due to electrostatic repulsive and van der Waals attractive forces must be considered. It has been recognized that these forces play an important part in colloid chemistry, particularly in relationship to aggregation and disaggregation [9,10].

In SdFFF, the stability of a colloidal system is provided by repulsive interactions originating in the surface charge on the particles and the electrical properties of the surface of the flow channel. The adsorption of colloidal particles onto the channel wall will be suppressed or promoted due to charge–charge interaction between the particles and the wall. The solution ionic strength is a factor effecting these forces and the resultant stability.

Opposing the electrostatic repulsive forces are the van der Waals attractions. Although these are directly independent of solution ionic strength and dependent most strongly on the dielectrical properties of the materials and of the involved carrier solution, as well as on the closest distance of the particles from the wall, these are indirectly dependent on the suspension's ionic strength, as the latter strongly influences the gap width between the planar wall and the closest particle's surface in SdFFF.

The potential barrier field flow fractionation (PBFFF) technique consists of changing the total potential energy of interaction between the colloidal particles and the material of the SdFFF channel wall by changing the ionic strength of the carrier solution from a high value, where colloidal particles are totally adhered at the beginning of the FFF channel wall, to a lower value, where the total number of adhered particles is released [11–18].

The method has been applied successfully to the size fractionation and characterization of monodisperse submicron particles of hematite and titanium dioxide [11–14],

of polymethylmethacrylate (PMMA) [15] and of various supramicron polydisperse irregular particles of mixed sulfides [16,17]. The same technique was also used for the concentration and size characterization of dilute colloidal samples, in both the normal and the steric modes of operation in SdFFF [13,18].

The purpose of the present work is to show the influence of the ionic strength of the suspending medium into the space constant of the exponential transverse concentration distribution l of the analyte compressed against the accumulation wall of the FFF channel, and consequently the influence of the l parameter to the total potential energy of interaction between the colloidal particles and the channel wall. From the later influence, the total potential energy of interaction between the colloidal particles and the channel wall at various particle–wall distances can be estimated.

2. Experimental

The experimental procedure has been described in detail elsewhere [19,20]. In this work, a SdFFF system has been used with the following dimensions: $37.4 \, cm \times 2.35 \, cm \times 0.017 \, cm$ with a channel void volume of $1.49 \, cm^3$, measured by the elution of the non-retained peak of sodium benzoate. The column had a radius of 6.85 cm from the center of rotation. The material of the accumulation wall was of the type Hastelloy-C, which is principally Ni (56%) with 15% Cr, 17% Mo, 5% Fe, 4% W, and traces of Mn and Si.

Triply distilled, CO_2-free water, containing 0.1% (v/v) of the low foaming, low alkalinity, phosphate, chromate and silicate-free detergent FL-70 (Fisher Scientific Company, Fairlawn, NJ 07410, USA), a mix of anionic and nonionic surfactants, and 0.02% (w/v) sodium azide as bacteriocide has been employed as carrier.

The electrolyte added to the carrier solution in order to adjust its ionic strength was potassium nitrate (KNO_3) 99.0% pure from Riedel-de Haën (D-30926 Seelze, Germany). The concentration of the added electrolyte ranged from 1.0×10^{-3} to $1.6 \times 10^{-1} \, M \, KNO_3$. The ionic strength of FL-70 alone was taken to be 1.0×10^{-3} from conductivity measurements. The pH of the suspending medium was constant and roughly equal to 9.0, as it was measured by the 744 pH-meter model of Ω Metrohm.

Silica (silicon dioxide, SiO_2) monodisperse colloidal particles from Duke Scientific Corporation with nominal diameter of $0.47 \pm 0.03 \, \mu m$ and microsphere density of $1.83 \, g \, cm^{-3}$ were used as sample. The silica particles were dispersed in the carrier liquid and sonicated for 2 min as a further aid to particle dispersion. Injection of $20 \, \mu L$ volume of the silica suspension was made into the channel by a microsyringe. Following injection, the longitudinal flow ($=150 \, mL \, h^{-1}$) was stopped for 4 min to allow for sample relaxation. The appropriate field strength for silica particles used was 300 rpm ($67.58 \, m \, s^{-2}$).

For comparison purposes scanning electron micrographs of the silica particles dispersed in different media were obtained by using a JEOL JSM-5200 scanning electron microscope (SEM) from JEOL (Tokyo, Japan).

3. Results and discussion

It has been shown that the mean thickness l of the cloud of particles compressed against the accumulation wall of the FFF channel influences rapidly the time needed to generate one theoretical plate [21–23] and the velocity of the particle zone [24]. Thus, by reducing the l value it would be possible to gain maximum speed for the elution/separation of colloidal particles. This reduction has been succeeded by several experimental conditions and various programming methods [25,26] as the field programming and the flow programming techniques, as well as the dual stream splitter system [21]. However, decreasing l values results to increasing particle–wall interactions [27], which leads to several complications that must be overcome. Due to the last observation, the reverse procedure could be followed and the l parameter could be decreased by increasing the particle–wall interactions. According to PBFFF this could be succeed by changing the total potential energy of interaction, V, between a spherical particle and the channel wall. In the present work, the variation of the total potential energy was due to the variation of the concentration of the electrolyte added to the carrier liquid. Fig. 1 illustrates four fractograms obtained by SdFFF at different values of ionic strength of the carrier solution. Fig. 1(a) shows a symmetrical peak corresponding to SiO_2 when the carrier solution does not contain any amount of electrolyte ($I = 1.0 \times 10^{-3} \, M$).

While the ionic strength increases, the particle wall interactions become significant and a broadening of the resolution peak appears [cf. Fig. 1(b) and (c)]. At high values of ionic strength ($1.6 \times 10^{-1} \, M$) the total amount of the colloidal particles are adhered at the beginning of the channel wall [cf. Fig. 1(d)]. Variation of the carrier solution to one with lower ionic strength ($1.0 \times 10^{-3} \, M$) released all the adherent particles [cf. Fig. 1(d)]. The corresponding diameters for the silica particles are given in Table 1. The variation of the ionic strength entails a positive deviation of the particle's diameter from that expected by the normal SdFFF theory, $\Delta d = d_{app} - d_{true}$, which is almost steady in the range of ionic strength from 1.0×10^{-1} to $1.5 \times 10^{-1} \, M$ (cf. Fig. 2). The later indicates that high values of ionic strength are suitable to compress the double layer and to eliminate the electrostatic repulsion. Therefore, in the used variation of the electrolyte concentration, the interaction forces between the particles and the wall in PBFFF could be converted from repulsive to attractive ones and vice versa. One could assume that this predominance of the attractive forces would lead to coagulation of the SiO_2 particles. However, these phenomena are absent according to the SEM pictures were obtained, as they are represented in Fig. 3.
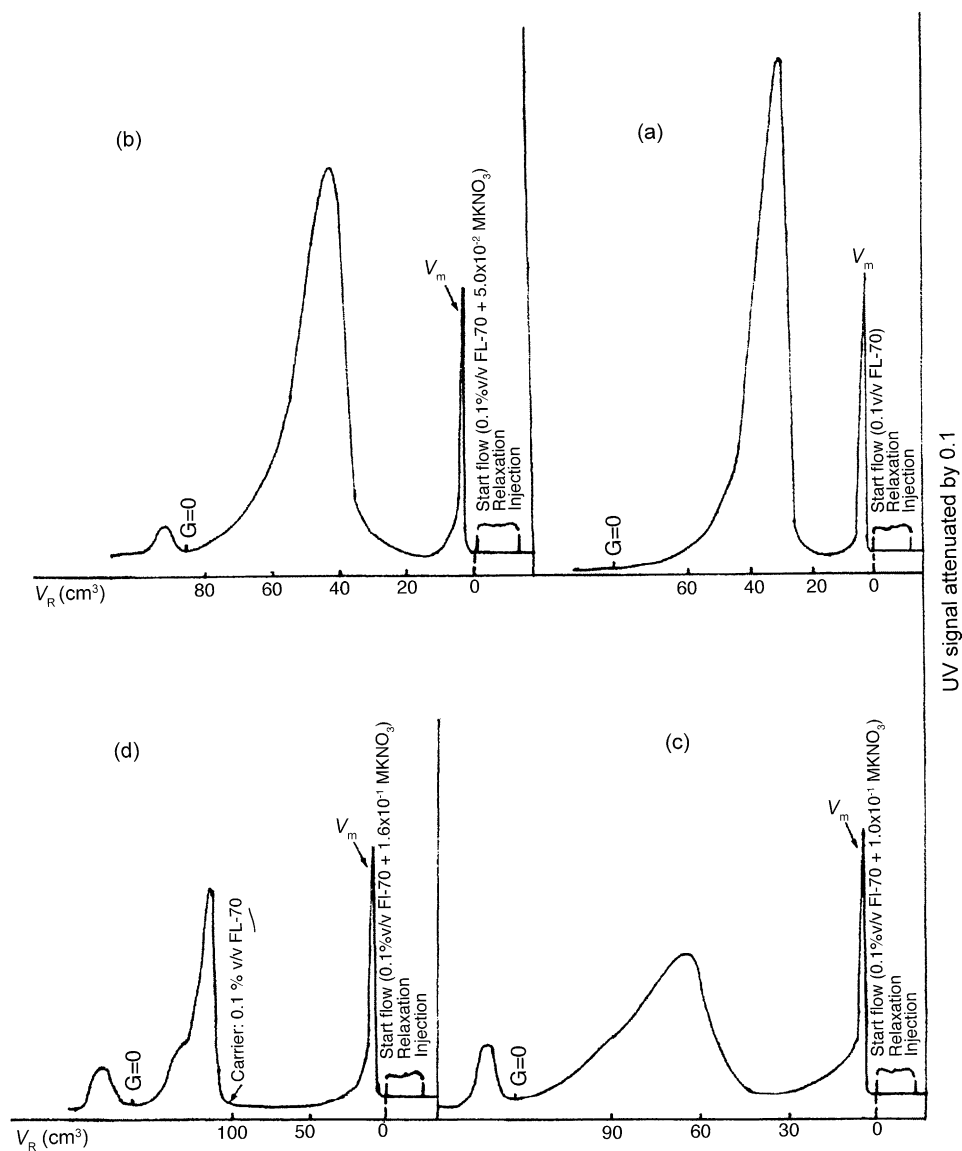
Fig. 1. Fractograms of SiO_2 colloidal particles at various ionic strengths of the suspending medium obtained by SdFFF. (a) $I = 1.0 \times 10^{-3}$, (b) $I = 5.0 \times 10^{-2}$, (c) $I = 1.0 \times 10^{-1}$, (d) $I = 1.6 \times 10^{-1}$.

Although no aggregation phenomena exist, gelatinization of the electrolyte appears at high ionic strength ($I > 1.6 \times 10^{-1}$ M), where is even possible to distinguish the individual regions with the parallel orientation. This can justify the fact that when we change the carrier solvent from the one with high ionic strength to that with no electrolyte added, the deposed silica particles are released immediately, as it can be shown from the corresponding fractogram in Fig. 1(d). It is possibly due to the same fact that all the adherent particles are not released, as it is obvious from the peak that appears after the interruption of the externally applied field.

In order to test the precision of the SdFFF method in measuring particles' diameters and to show whether the observed variation of the apparent diameter with the suspension's ionic strength is statistically significant, various

SdFFF experiments in the absence of electrolyte were performed. The obtained results are presented in Table 2, from which the precision of the method is computed to be 98.2% [$=100 - (0.009/0.496)100$].

Test of significance between the found mean diameter (d_m) and that given by manufacturer (d_n) shows that these values are not statistically different, thus making possible the accurate determination of the diameters for the SiO_2 particles. Therefore, *accurate* and *precise* diameters of the SiO_2 particles can be determined by SdFFF.

When the particle-wall interactions are absent in SdFFF, the potential energy of a spherical particle, V_{SdFFF}, is given by the relation [12]:

$$V_{SdFFF} = \frac{4}{3}\pi a_{true}^3 \Delta\rho G_{SdFFF}x \qquad (1)$$

Table 1
Apparent diameters, d_{app}, of SiO₂ particles determined by SdFFF at various ionic strengths, I, of the suspending medium

I (M)	d_{app} (μm)
1.0×10^{-3}	0.496
3.0×10^{-3}	0.502
5.0×10^{-3}	0.511
6.0×10^{-3}	0.512
7.0×10^{-3}	0.516
8.0×10^{-3}	0.511
9.0×10^{-3}	0.515
1.0×10^{-2}	0.511
2.0×10^{-2}	0.521
3.0×10^{-2}	0.525
4.0×10^{-2}	0.538
5.0×10^{-2}	0.566
6.0×10^{-2}	0.585
7.0×10^{-2}	0.598
8.0×10^{-2}	0.606
9.0×10^{-2}	0.628
1.0×10^{-1}	0.674
1.1×10^{-1}	0.678
1.3×10^{-1}	0.671
1.4×10^{-1}	0.670
1.5×10^{-1}	0.679
1.6×10^{-1}	Total adhesion

where a_{true} is the true particle diameter when the particle–wall interactions are absent, which can be determined by SdFFF in the absence of electrolyte, Δp is the density difference between the particle and the carrier, G_{SdFFF} ($\sim 67.58\,\text{m s}^{-2}$, 300 rpm) is the constant sedimentation field expressed as acceleration and x is the coordinate position of the center of particle mass, which in our case is the effective mean cloud thickness, l_{eff}, given by the equation

$$l_{eff} = l_{app} - a_{true} \tag{2}$$

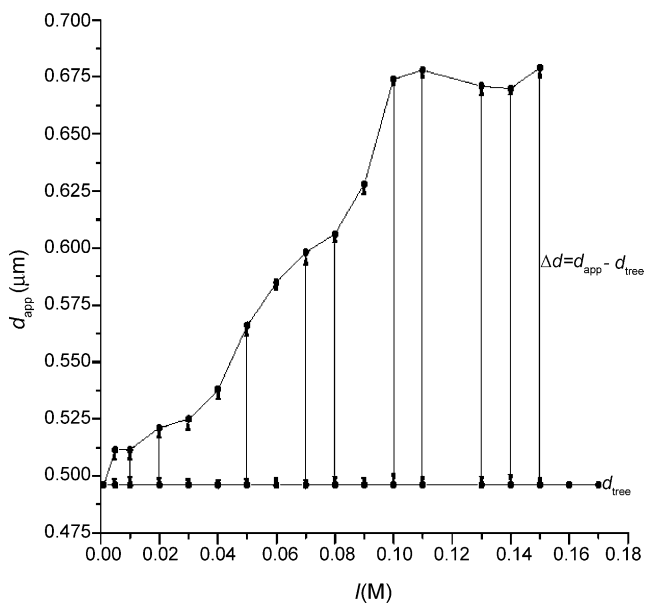
Fig. 2. Variation of the apparent particle diameter (d_{app}) of the silica particles with the ionic strength (I) of the carrier solution.

Table 2
Silica particles' diameters (d) determined by various SdFFF experiments in the absence of electrolyte, the mean diameter of these values (d_m) with the corresponding standard deviation (σ_{d_m}) and the nominal particle diameter (d_n) with its standard deviation (σ_{d_n}) given by the manufacturer

Number of experiment	d (μm)	$d_m \pm \sigma_{d_m}$ (μm)	$d_n + \sigma_{d_n}$ (μm)
1	0.498		
2	0.490		
3	0.487		
4	0.487		
5	0.484	0.496 ± 0.009	0.470 ± 0.030
6	0.499		
7	0.502		
8	0.506		
9	0.502		
10	0.509		

l_{app} is the apparent mean cloud thickness in SdFFF, which can be computed from the known relation [1]:

$$l_{app} = \frac{Rw}{6} = \frac{V_0 w}{6V_r} = \frac{6kT}{\pi d_{app}^3 \Delta \rho G_{SdFFF}} \tag{3}$$

where R is the retention ratio, V_0 is the void volume of the channel, V_r is the particle's retention volume, w is the channel thickness and d_{app} is the apparent particle diameter determined at various ionic strengths. Therefore, Eq. (1) can be written as:

$$V_{SdFFF} = \tfrac{4}{3}\pi a_{true}^3 \Delta \rho G_{SdFFF} l_{eff} \tag{4}$$

In the case when the colloidal particles interact with the SdFFF channel wall, the potential energy given by Eq. (4) must be corrected by considering the potential energy of interaction, V_{int}. The latter, in the absence of chemical bonds, can be estimated by the sum of the contribution of the van der Waals attractive, V_A, and the double-layer repulsive, V_R, energies:

$$V_{int} = V_A + V_R \tag{5}$$

The total potential energy, V_{tot}, of a spherical particle in SdFFF will equal the sum of Eqs. (1) and (5):

$$V_{tot} = V_{SdFFF} + V_{int} \tag{6}$$

The V_{tot} could be expressed in terms of an apparent sedimentation field strength, G_{app}, which varies with the solution ionic strength, by considering a relation analogous to Eq. (4):

$$V_{tot} = \tfrac{4}{3}\pi a_{true}^3 \Delta \rho G_{app} l_{eff} \tag{7}$$

The G_{app} value can be computed from the relation:

$$G_{app} = \frac{6kT}{\pi d_{true}^3 \Delta \rho l_{app}} \tag{8}$$

where $d_{true} = 496\,\text{nm}$ is the particle diameter determined by SdFFF when the carrier solution is triply distilled water with 0.1% (v/v) FL-70 as a surfactant and 0.02% (w/v) sodium azide as bacteriocide, i.e. when the particle–wall interactions are absent.
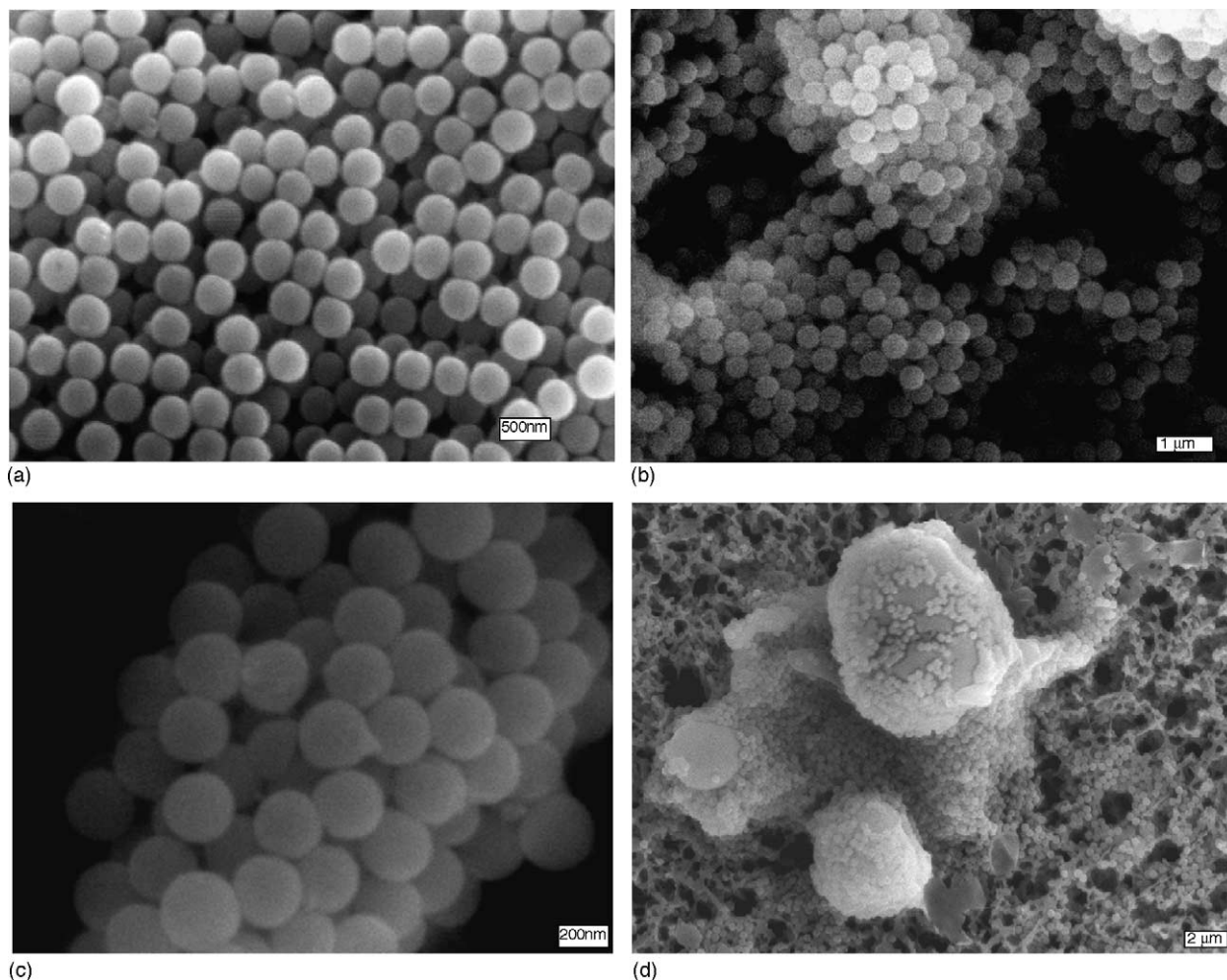
Fig. 3. SEM pictures of the colloidal silica particles at various ionic strengths of the carrier solution. (a) $I = 1.0 \times 10^{-3}$, (b) $I = 5.0 \times 10^{-2}$, (c) $I = 1.0 \times 10^{-1}$, (d) $I = 1.6 \times 10^{-1}$.

Combination of Eqs. (4), (6) and (7) gives the V_{int}:

$$V_{int} = \tfrac{4}{3}\pi a_{true}^3 \Delta\rho(G_{app} - G_{SdFFF})l_{eff} \qquad (9)$$

The experimental values of l_{app}, l_{eff} and G_{app} calculated from Eqs. (3), (2) and (8), respectively, at various ionic strengths of the carrier, are compiled in Table 3.

Eq. (9) can be simply used to estimate the V_{int} values from two SdFFF experiments, one with carrier solution without any amount of electrolyte, and the second with a carrier solution having a given electrolyte amount, as given below.

From the first experiment, the experimental parameters V_0, V_r and the known values of Δp and G_{SdFFF}, the l_{app}, l_{eff} and a_{true} (=248 nm) values are computed with the aid of Eqs. (2) and (3), from which the V_{SdFFF} is estimated via Eq. (4).

From the second experiment, in the presence of a given amount of electrolyte (KNO_3), the l_{app} value is estimated from Eq. (3) from which the G_{app} is calculated via Eq. (8) using as d_{true} that calculated in the first experiment. Finally, the V_{int} is estimated with the aid of Eq. (9).

The values of V_{int}^{exp} found by the proposed method of SdFFF are compared with those calculated theoretically, V_{int}^{th}, from Eq. (5) using as V_A and V_R the various forms of the equations predicted by the Derjaguin–Landau–Verwey–Overbeek (DLVO) theory. As the distances of the silica particles from the channel wall are too high (900.21 nm > l_{eff} > 199.56 nm) in all of our cases, the van der Waals attractive energy, V_A, predominates to the double-layer repulsive ones, V_R, thus making possible the approximation of V_{int} with the V_A values: $V_{int} \cong V_A$.

The van der Waals particle–wall interaction energy, V_A, which depends on the particle diameter and the distance from the wall, l_{eff}, can be calculated from the following equations [28–29]:

$$V_A \cong V_{int}^{th} \cong -\frac{4}{3}\frac{A_{132}d^3}{kT(4l_{eff}^2 - d^2)^2}l_{eff} \qquad (10)$$

$$V_A \cong V_{int}^{th} \cong -\frac{A_{132}}{kT}\left[\ln\frac{l_{eff}+d}{l_{eff}} - \frac{d(l_{eff}+d/2)}{l_{eff}(l_{eff}+d)}\right] \qquad (11)$$

Table 3
Variation of the apparent mean cloud thickness, l_{app}, the effective cloud thickness, l_{eff}, and the apparent sedimentation field strength, G_{app}, with the ionic strength, I, of the suspending medium

I (M)	l_{app} (nm)	l_{eff} (nm)	G_{app} (m s^{-2})
1.0×10^{-3}	1148.21	900.21	67.58
3.0×10^{-3}	1107.52	859.52	70.07
5.0×10^{-3}	1050.03	802.03	73.90
6.0×10^{-3}	1043.89	795.89	74.34
7.0×10^{-3}	1019.80	771.80	76.09
8.0×10^{-3}	1050.03	802.03	73.90
9.0×10^{-3}	1025.76	777.76	75.65
1.0×10^{-2}	1050.03	802.03	73.90
2.0×10^{-2}	980.99	732.99	79.10
3.0×10^{-2}	958.80	710.80	80.93
4.0×10^{-2}	891.14	643.14	87.08
5.0×10^{-2}	765.67	517.67	101.35
6.0×10^{-2}	693.70	445.70	111.86
7.0×10^{-2}	649.60	401.60	119.46
8.0×10^{-2}	624.31	376.31	124.30
9.0×10^{-2}	561.22	313.22	138.27
1.0×10^{-1}	457.60	209.60	169.58
1.1×10^{-1}	449.55	201.55	172.62
1.3×10^{-1}	463.76	215.76	167.33
1.4×10^{-1}	465.84	217.84	166.58
1.5×10^{-1}	447.56	199.56	173.38
1.6×10^{-1}	Total adhesion	Total adhesion	Total adhesion

where A_{132} is the effective Hamaker constant for media 1 (Hastelloy-C) and 2 (SiO$_2$) interacting across medium 3 (carrier solution), which can be estimated from the relation [30]:

$$A_{132} = (A_{11}^{1/2} - A_{33}^{1/2})(A_{22}^{1/2} - A_{33}^{1/2}) \tag{12}$$

In the last equation, A_{ii} are Hamaker constants for two bodies of material i interacting in vacuum. In fact, A_{132} is not truly a constant, as its value decreases at large particle - wall distances due to a retardation effect. Eqs. (10) and (11) can be used to calculate the V_{int}^{th} values using as A_{132} the value 1.02×10^{-20} J given in literature [29]. The experimental potential energies of interaction, V_{int}^{exp}, between SiO$_2$ particles and the channel wall determined by Eq. (9) and those calculated from Eqs. (10) and (11) at various ionic strengths of the carrier solution are presented in Table 4.

The deviation of the determined V_{int}^{exp} from those calculated from Eqs. (10) and (11) can be attributed either to the retardation effect [8] which has been neglected from the latter equations, although it is significant at the used large separations (900.21 nm > l_{eff} > 199.56 nm), or to the fact that in Eqs. (10) and (11) the A_{132} is supposed to be constant in the whole range of solution's ionic strength. Better agreement, at the lower ionic strengths, e.g. at the larger distances of the particles from the wall, appears when we use Eq. (10) which is valid at relatively large separation distances. On the other hand, at the higher ionic strengths the agreement is better when we use Eq. (11), which is more accurate at small distances of the particles from the wall. Concerning the suspension's ionic strength, the experimental V_{int}^{exp} values are closer to those calculated from the empirical equations when it is lower than 0.05, due to the reason that at higher

Table 4
Experimental potential energies of interaction between the SiO$_2$ particles and the channel wall (V_{int}^{exp} in kT units) determined by SdFFF, as well as corresponding theoretical values (V_{int}^{th} in kT units) calculated from various empirical equations at different ionic strengths (I) of the suspending medium

I (M)	V_{int}^{exp} (kT)	V_{int}^{th} (kT)	
		Eq. (10)	Eq. (11)
1.0×10^{-3}	0	0	0
3.0×10^{-3}	−0.027	−0.0473	−0.00657
5.0×10^{-3}	−0.065	−0.0597	−0.00777
6.0×10^{-3}	−0.070	−0.0609	−0.00791
7.0×10^{-3}	−0.085	−0.0678	−0.00852
8.0×10^{-3}	−0.065	−0.0597	−0.00777
9.0×10^{-3}	−0.080	−0.0658	−0.00836
1.0×10^{-2}	−0.065	−0.0597	−0.00777
2.0×10^{-2}	−0.108	−0.0823	−0.00963
3.0×10^{-2}	−0.123	−0.0909	−0.0104
4.0×10^{-2}	−0.162	−0.131	−0.0131
5.0×10^{-2}	−0.225	−0.306	−0.0214
6.0×10^{-2}	−0.254	−0.597	−0.0296
7.0×10^{-2}	−0.269	−1.02	−0.0370
8.0×10^{-2}	−0.275	−1.48	−0.0424
9.0×10^{-2}	−0.285	−5.89	−0.0616
1.0×10^{-1}	−0.276	−17.1	−0.132
1.1×10^{-1}	−0.273	−11.6	−0.142
1.3×10^{-1}	−0.277	−24.3	−0.126
1.4×10^{-1}	−0.278	−27.8	−0.123
1.5×10^{-1}	−0.271	−10.7	−0.145
1.6×10^{-1}	Total adhesion	Total adhesion	Total adhesion

ionic strengths the particle–particle interactions may be also appreciable. The fact that the calculated V_{int}^{th} values from various empirical equations deviate significantly, explains the dispersion of our V_{int}^{exp} values, as well as their deviation from all theoretical values.

4. Conclusion

The main advantages of the proposed SdFFF method are the following:

(1) Estimation of the total potential energy of interaction from two simple SdFFF experiments at different suspension's ionic strength. The only needed experimental parameters are the density of the particles and of the medium and the acceleration field strength. The total potential energy of interaction, which is compatible with that calculated from various empirical equations, can be determined at every suspension's ionic strength, e.g. at every distance of the particles from the channel wall. The agreement between theory and experimental results is very good considering the approximate nature of the parameters used.
(2) Values of the Hamaker constants, which cannot be determined easily and accurately, are not necessary.
(3) Values of the surface potentials of the particles and the channel wall are not necessary.

(4) From the total interactive energies, V_{int}^{exp}, determined in the present work and using various empirical equations relating V_{int} with the effective Hamaker constants, A_{132}, the latter can be determined with a simple and accurate way. The dependence of A_{132} on suspension's ionic strength can be also studied with simplicity and accuracy.

Acknowledgements

References

[1] K.D. Caldwell, in: H.G. Barth (Ed.), Modern Methods of Particle Size Analysis, John Wiley and Sons, New York, 1984 (Chapter 7).
[2] J. Janca, Field Flow Fractionation, Marcel Dekker, New York, 1987.
[3] J.C. Giddings, Sep. Sci. Technol. 1 (1966) 123.
[4] Y. Mori, K. Kimura, M. Tanigaki, Anal. Chem. 62 (1990) 2668.
[5] J.C. Giddings, F.J.F. Yang, M.N. Myers, Sep. Sci. Technol. 10 (1975) 133.
[6] J.C. Giddings, M.N. Myers, F.J.F. Yang, L.K. Smith, in: M. Kerker (Ed.), Colloid and Interface Science, vol. IV, Academic Press, New York, 1976, p. 381.
[7] J.C. Giddings, M.N. Myers, J.F.J. Moellmer, Chromatographia 149 (1978) 501.
[8] M.E. Hansen, J.C. Giddings, Anal. Chem. 61 (1989) 811.
[9] E. Matijevic, Surface and Colloidal Science, vol. 8, Wiley, New York, 1976 (Chapter 1).
[10] D.J. Shaw, Introduction to Colloid and Surface Chemistry, Butterworths, London, 1980.
[11] G. Karaiskakis, A. Koliadima, Chromatographia 28 (1989) 31.
[12] A. Koliadima, G. Karaiskakis, J. Chromatogr. 517 (1990) 345.
[13] A. Koliadima, G. Karaiskakis, Chromatographia 39 (1994) 74.
[14] G. Karaiskakis, A. Athanasopoulou, A. Koliadima, J. Microcolumn Sep. 9 (1997) 275.
[15] G. Karaiskakis, M. Douma, I. Katsipou, A. Koliadima, L. Farmakis, J. Liq. Chromatogr. Relat. Technol. 23 (2000) 1953.
[16] A. Athanasopoulou, G. Karaiskakis, Chromatographia 40 (1995) 734.
[17] A. Athanasopoulou, G. Karaiskakis, Chromatographia 43 (1996) 369.
[18] G. Karaiskakis, in: J. Cazes (Ed.), Encyclopedia of Chromatography, Marcel Dekker Inc, New York, 2001, p. 653.
[19] E. Dalas, G. Karaiskakis, Colloids Surf. 28 (1987) 169.
[20] E. Dalas, P. Koutsoukos, G. Karaiskakis, Colloid Polym. Sci. 268 (1990) 155.
[21] J.C. Giddings, Anal. Chem. 57 (1985) 945.
[22] J.C. Giddings, Sep. Sci. Technol. 8 (1973) 567.
[23] J.C. Giddings, M. Martin, M.N. Myers, J. Chromatogr. 158 (1978) 419.
[24] J.C. Giddings, M.N. Myers, K.D. Caldwell, S.R. Fisher, in: D. Glick (Ed.), Methods of Biochemical Analysis, Wiley, New York, 1980, p. 79.
[25] F.J.F. Yang, M.N. Myers, J.C. Giddings, Anal. Chem. 46 (1974) 1924.
[26] J.C. Giddings, K.D. Caldwell, Anal. Chem. 56 (1984) 2093.
[27] M.N. Myers, J.C. Giddings, Anal. Chem. 54 (1982) 2284.
[28] M. Martin, J. Chromatogr. A 831 (1999) 73.
[29] G. Karaiskakis, A. Koliadima, L. Farmakis, D. Gavril, J. Liq. Chromatogr. Relat. Technol. 25 (2002) 2153.
[30] J.N. Israelachvili, Intermolecular and Surface Forces, Academic Press, London, 1987, p. 144.